(41) N. Sutin, "Inorganic Biochemistry", G. Eichorn, Ed., Elsevier, Amsterdam, 1973, Chapter 19.
(42) M. J. Powers and T. J. Meyer, *J. Am. Chem. Soc.*, **100**, 4393 (1978).
(43) Theoretical treatments indicate that both the electronic transmission coefficient and nuclear tunneling effects contribute to $\langle\kappa\rangle$. The latter effect is expected to reflect itself in ΔH^*.
(44) J. L. Cramer and T. J. Meyer, *Inorg. Chem.*, **13**, 1250 (1974).
(45) J. N. Braddock and T. J. Meyer, *J. Am. Chem. Soc.*, **95**, 3158 (1973).
(46) From a consideration of the equation $k = \langle\kappa\rangle(k_BT/h)\exp[-\Delta H^*/RT + \Delta S^*/R]$ a value of $\langle\kappa\rangle$ was calculated by equating the excess entropy of activation to $R \ln \langle\kappa\rangle$.
(47) N. Sutin, *Acc. Chem. Res.*, **1**, 225 (1968).

Contribution from the Department of Chemistry, University of Calgary, Calgary, Alberta, Canada T2N 1N4

Synthesis and Structure of Salts of the Bicyclic Sulfur–Nitrogen Cation $S_4N_5^+$ and a Comparison of the Electronic Structures of the Tetrasulfur Pentanitride(1+) and -(1-) Ions

T. CHIVERS,* L. FIELDING, W. G. LAIDLAW, and M. TRSIC

Received July 12, 1979

The new sulfur–nitrogen halide S_4N_5Cl has been prepared in good yield from trithiazyl trichloride, $S_3N_3Cl_3$, and bis[(trimethylsilyl)imido]sulfur, $Me_3SiN{=}S{=}NSiMe_3$, in carbon tetrachloride. An X-ray structural determination of this compound shows it to have a polymeric, predominantly ionic, structure in which bicyclic $S_4N_5^+$ cations are symmetrically bridged by Cl^- ions. Crystals of S_4N_5Cl are orthorhombic and belong to the space group *Pnma* with a = 17.491 (17) Å, b = 7.819 (2) Å, and c = 4.838 (4) Å, V = 661.7 (5) Å^3, Z = 4, and D_c = 2.346 g cm^{-3}. The structure was solved by direct methods and Fourier techniques and refined to a conventional R factor of 0.066 for 1162 independent reflections with $I \geq 3\sigma(I)$. The reaction of S_4N_5Cl with silver(II) fluoride or antimony pentachloride gives S_4N_5F or $S_4N_5SbCl_6$, respectively. The vibrational spectra of these salts of the $S_4N_5^+$ cation are reported. Ab initio Hartree–Fock–Slater SCF calculations have been carried out for $S_4N_5^+$ and for the related anion $S_4N_5^-$ in order to compare their ground-state electronic structures with that of S_4N_4, and, in particular, to assess the importance of S--S interactions within these S–N cages. These calculations show that the introduction of a bridging N^- entity into the S_4N_4 framework destroys one of the transannular S--S bonds and weakens the S–N framework bonds. In $S_4N_5^+$ there are no S--S bonds, as expected for loss of 2 electrons from the $S_4N_5^-$ anion.

Introduction

The growing number of binary S–N cations which have been structurally characterized attests to the rich diversity of this area of nonmetal chemistry. This list now includes NS^+,[1] NS_2^+,[2] $S_3N_2^+$,[3] $S_4N_3^+$,[4] $S_4N_4^{2+}$,[5] $S_5N_5^+$,[6] and $S_6N_4^{2+}$.[7] In a preliminary communication we described the synthesis and structure of S_4N_5Cl,[8] which contains the first bicyclic S–N cation, $S_4N_5^+$. In this paper we report the full details of the synthesis and spectroscopic characterization of three salts of the $S_4N_5^+$ ion. In addition, we have carried out ab initio Hartree–Fock–Slater (HFS) SCF calculations of the ground-state electronic structures of $S_4N_5^+$ and the related anion $S_4N_5^-$,[9] in order to assess the effect of introducing an N^- or N^+ species into the S_4N_4 framework with particular reference to the importance of transannular S--S interactions in these S–N cages.

Experimental Section

General Procedures. All experiments were performed under dry nitrogen (Linde 99.998% passed through silica gel) in oven-dried glassware. Manipulations involving air-sensitive compounds were carried out in a Vacuum Atmospheres drybox. Carbon tetrachloride and methylene chloride were stored over P_2O_5 and distilled before use. $S_3N_3Cl_3$[10] and $Me_3SiNSNSiMe_3$[11] were prepared by standard literature procedures. Thionyl chloride, sulfuryl chloride, and antimony pentachloride were freshly distilled before use. All other chemicals were commercial samples used as received.

Infrared spectra (4000–250 cm^{-1}) were recorded as Nujol mulls on a Perkin-Elmer 467 spectrophotometer using CsI windows. Raman spectra were obtained on samples sealed in capillaries under nitrogen by using a He/Ne (6328 Å) laser and a Jarrell-Ash spectrophotometer and were calibrated against carbon tetrachloride. UV–visible spectra were recorded on a Cary 15 spectrometer. Mass spectra were recorded on a Varian CH5 spectrometer operating at 70 eV. Elemental analyses were performed by the Analytische Laboratorien, Engelskirchen, West Germany.

Preparation of S_4N_5Cl. $Me_3SiNSNSiMe_3$ (0.83 g, 4.03 mmol) was added to a stirred solution of $S_3N_3Cl_3$ (0.95 g, 3.88 mmol) in carbon tetrachloride (55 mL), which had been filtered through a fine glass frit. The solution was allowed to stand at 23 °C for 12 h, whereupon the supernatant liquid was decanted by pipet from the crystalline product. The golden green crystals were washed with carbon tetrachloride and dried in vacuo for 20 min to give tetrasulfur pentanitride chloride, mp 108 °C (0.56 g, 2.40 mmol, 62% yield). Anal. Calcd for S_4N_5Cl: S, 54.86; N, 29.97; Cl, 15.17. Found: S, 54.58; N, 29.97; Cl, 15.23.

Removal of solvent from the decanted solution produced a further 0.16 g of S_4N_5Cl as a yellow powder. The crystals obtained above were found to be suitable for the X-ray structural determination described below. In preparations in which the solution of reagents was stirred during the reaction, the product was obtained as a yellow powder.

Caution! Like all nitrogen-rich S–N species, S_4N_5Cl is potentially explosive and care should be exercised to avoid subjecting samples to friction or sudden heating.

Preparation of S_4N_5F. An excess of silver difluoride (1.57 g, 10.7 mmol) was stirred with a solution of S_4N_5Cl (0.26 g, 1.10 mmol) in methylene chloride (15 mL). The yellow solution turned green and effervesced for the first 10 min. After 13 h, the solution was decanted from the black residue (1.56 g) and solvent was removed by slow vacuum transfer at −78 °C. When the volume was ca. 4 mL, the supernatant liquid was decanted to give dark green crystals of S_4N_5F (0.15 g, 6.91 mmol, 63%), which were dried in vacuo for 15 min. Anal. Calcd for S_4N_5F: S, 59.02; N, 32.23; F, 8.74. Found: S, 58.70; N, 32.09; F, 8.59.

Removal of solvent from the decanted solution produced a further 0.05 g of S_4N_5F.

Preparation of $S_4N_5SbCl_6$. A solution of antimony pentachloride (0.50 g, 1.68 mmol) in methylene chloride (3.5 mL) was slowly added to a clear yellow solution of S_4N_5Cl (0.34 g, 1.48 mmol) in methylene chloride (25 mL). A yellowish precipitate, which formed immediately, was filtered off, washed with methylene chloride (20 mL), dried in vacuo for 30 min, and identified as $S_4N_5SbCl_6$ (0.56 g, 1.07 mmol, 73% yield). Anal. Calcd for $S_4N_5Cl_6$: S, 24.07; N, 13.15; Cl, 39.93. Found: S, 23.77; N, 13.28; Cl, 40.08.

Crystal Data for S_4N_5Cl. Golden prisms suitable for X-ray diffraction studies were obtained as described above. The dimensions of the crystal used in this study were 0.25 × 0.25 × 0.28 cm. All

0020-1669/79/1318-3379$01.00/0

Table I. Positional and Thermal Parameters[a] for S_4N_5Cl and Their Estimated Standard Deviations

atom	x	y	z	B_{11}	B_{22}	B_{33}	B_{12}	B_{13}	B_{23}
Cl	0.1317 (1)	0.7500 (0)	0.5811 (5)	0.00220 (7)	0.1331 (9)	0.0231 (9)	0.0000 (0)	−0.0011 (5)	0.0000 (0)
S(1)	0.2063 (1)	0.2500 (0)	0.4142 (5)	0.00180 (7)	0.0093 (4)	0.0161 (7)	0.0000 (0)	−0.0005 (4)	0.0000 (0)
S(2)	0.0484 (1)	0.2500 (0)	0.4756 (4)	0.00181 (7)	0.0075 (3)	0.0131 (7)	0.0000 (0)	0.0001 (4)	0.0000 (0)
S(3)	0.1107 (1)	0.5062 (2)	0.1566 (3)	0.00276 (5)	0.0076 (2)	0.0179 (5)	0.0000 (2)	0.0011 (3)	0.0068 (7)
N(1)	0.1320 (5)	0.2500 (0)	0.620 (1)	0.0021 (3)	0.0090 (12)	0.012 (3)	0.0000 (0)	−0.001 (1)	0.000 (0)
N(2)	0.1966 (3)	0.4173 (7)	0.201 (1)	0.0020 (2)	0.0082 (8)	0.020 (2)	−0.0007 (7)	0.002 (1)	0.001 (2)
N(3)	0.0439 (3)	0.4143 (7)	0.250 (1)	0.0024 (2)	0.0076 (8)	0.022 (2)	0.0002 (8)	−0.002 (1)	0.002 (3)

[a] The form of the anisotropic thermal parameters is $\exp[-(B_{11}h^2 + B_{22}k^2 + B_{33}l^2 + B_{12}hk + B_{13}hl + B_{23}kl)]$.

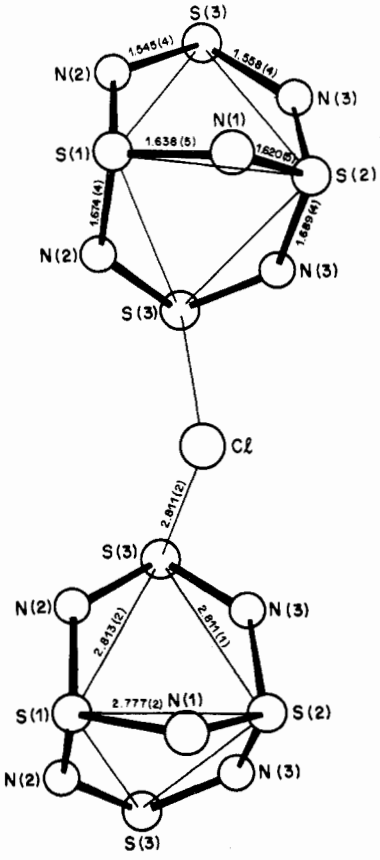

Figure 1. Structure of S_4N_5Cl showing principal interatomic distances in angstroms with esd's in parentheses.

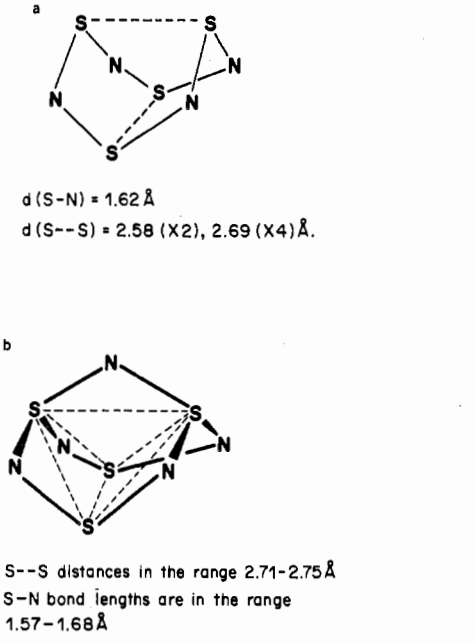

Figure 2. Structures of (a) S_4N_4 and (b) $S_4N_5^-$. Data were taken from ref 27a and 9, respectively.

manipulations were carried out under an atmosphere of dry nitrogen. The crystal was mounted in a glass capillary and the crystal orientation was random (mol wt 233.74; orthorhombic). For calculation of the cell constants, 25 reflections were computer centered and the setting angles were least-squares refined. The following systematic absences were observed: $0kl$, $k + l \neq 2n$; $hk0$, $h \neq 2n$. The cell constants are $a = 17.491$ (17) Å, $b = 7.819$ (2) Å, $c = 4.838$ (4) Å, and $V = 661.7$ (5) Å^3; $Z = 4$; $D_c = 2.346$ g cm^{-3}. The space group was *Pnma* or $Pna2_1$ (*Pnma* confirmed by refinement).

X-ray Measurements. Intensity data were collected at 23 ± 1 °C by using an Enraf-Nonius CAD4 diffractometer with graphite-monochromated Mo Kα radiation (λ 0.710 73 Å) and a θ–2θ scan rate varying from 4 to 20°/min, depending on the intensity of the reflection. Stationary-background counts with a time equal to half the scan time for each reflection were made at each end of the scan range. The scan range varied from −1.2° at low 2θ to +1.2° for the higher angle data. Of the 1222 reflections in the range $0° < 2\theta$(Mo Kα) $< 50°$, 1162 unique reflections with $I \geq 3\theta(I)$ were retained as observed and corrected for Lorentz and polarization effects. Three representative reflections were measured periodically to check crystal and electronic stability, but no significant change in intensity was observed. The linear absorption coefficient of this compound is 16.99 cm^{-1} for Mo Kα radiation and no absorption correction was necessary.

Solution and Refinement of the Structure. The structure was solved by direct methods. By use of reflections ($E_{min} = 1.40$) and 2000 phase relationships, a total of 16 phase sets were produced. With an E map prepared from the phase set showing the second best probability statistics (absolute figure of merit 0.854, residual 39.46) a total of four atoms were located. These atoms were included in least-squares refinement, resulting in agreement factors (defined below) of $R_1 = 0.38$ and $R_2 = 0.50$. The remaining nonhydrogen atoms were located in succeeding difference Fourier syntheses. All atoms were then refined anisotropically. The structure was found to lie on a crystallographic mirror plane.

In full-matrix least-squares refinement the function minimized was $\sum w(|F_o| - |F_c|)^2$ where the weight w is defined as $4F_o^2/\sigma^2(F_o^2)$. Scattering factors were taken from Cromer and Waber.[12] Anomalous dispersion effects were included in F_c; the values of $\Delta f'$ and $\Delta f''$ were those of Cromer and Liberman.[13] Only the 646 reflections having $F_o^2 > 3\sigma(F_o^2)$ were used in the refinement. The following values pertain to the final cycle of least-squares refinement: $R_1 = \sum||F_o| - |F_c||/\sum|F_o| = 0.066$; $R_2 = [\sum w(|F_o| - |F_c|)^2/\sum wF_o^2]^{1/2} = 0.087$. The final difference Fourier map showed no significant residual electron density. No unusual trends were observed in an analysis of $\sum w(|F_o| - |F_c|)^2$ vs. $|F_o|$, $\lambda^{-1}\sin\theta$, or various classes of indices. The positional and thermal parameters for S_4N_5Cl are given in Table I.

Calculations. Since S_4N_4 serves as a prototype for the systems of interest, $S_4N_5^-$ and $S_4N_5^+$, molecular orbital calculations were carried out for all three species. The experimentally determined geometry as shown in Figure 1 for $S_4N_5^+$ and in parts a and b of Figure 2 for S_4N_4 and $S_4N_5^-$, respectively, were used. With these geometries S_4N_4 transforms as D_{2d} and $S_4N_5^+$ and $S_4N_5^-$ transform as C_{2v}.

The self-consistent-field molecular orbitals (MO's) of the ground-state single determinant wave function for each molecule were calculated with use of a double-ζ (DZ) basis[14] augmented, for the sulfur atom, with a 3d orbital of exponent 1.68.[15] The HFS potential was used in a manner well described[16] and exemplified in the literature.[15,17,18] The $1s^2$ and $1s^22s^22p^6$ cores of nitrogen and sulfur, respectively, were kept "frozen" during the variational procedure as described and tested elsewhere.[15,16]

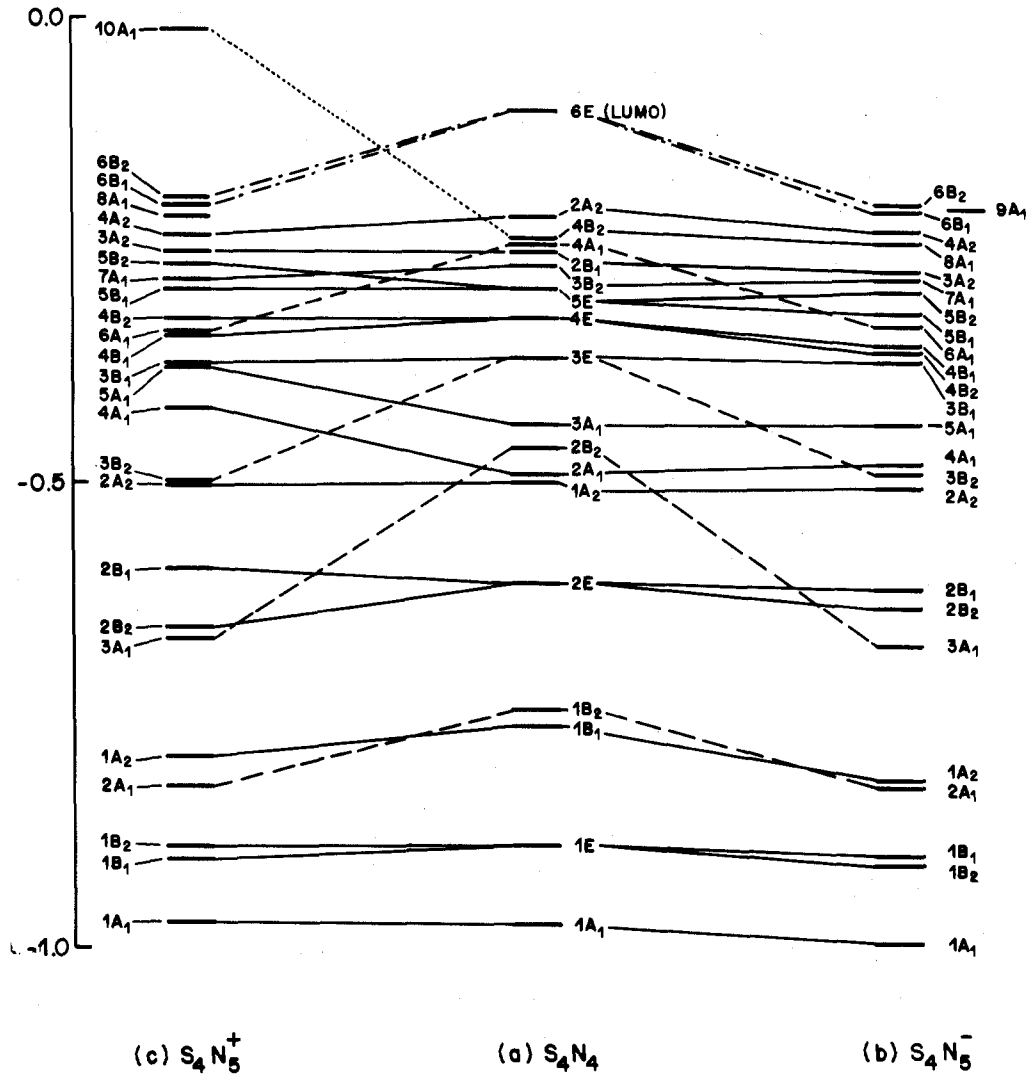

Figure 3. Energy level diagram for molecular orbitals in (a) S_4N_4 (D_{2d}), (b) $S_4N_5^-$, and (c) $S_4N_5^+$. The energy levels for $S_4N_5^+$ and $S_4N_5^-$ are shifted by +0.24 and −0.18, respectively, in order that the correspondence between systems is more apparent. The solid lines connect occupied orbitals which have essentially the same character; the dashed lines connect occupied orbitals which are strongly affected by insertion of N^+ or N^- into the S_4N_4 cage. The dash–dot or dot–dot lines involve orbitals which are, respectively, unoccupied in S_4N_4 (6E) or unoccupied in $S_4N_5^+$ ($10A_1$).

The energy level diagram for the three systems is given in Figure 3. In each case we calculated the total and per orbital overlap populations for the atom–atom regions of interest using well-known expressions.[19] These results are shown in Table V and Figure 4 together with the calculated atomic charge for each center.[19]

Results and Discussion

Synthesis of $S_4N_5^+$ Salts. Following the discovery of preparative routes to the S–N cage anion, $S_4N_5^-$,[20] we turned our attention to the synthesis of monofunctional derivatives of the S_4N_5 cage which might provide an opportunity to extend the number of cage atoms. The versatility of the reagent $Me_3SiN{=}S{=}NSiMe_3$ for the synthesis of S–N rings and cages by reaction with nonmetal halides is well documented,[21] and we therefore set out to prepare S_4N_5Cl by the reaction of this reagent with $S_3N_3Cl_3$, an S–N ring which is known to have a cis arrangement of the chlorine substituents.[22] The reaction proceeded smoothly at 23 °C in carbon tetrachloride to give S_4N_5Cl in good yield. S_4N_5Cl melts at 108 °C to give a clear red liquid which exploded violently after a few seconds. It is soluble in methylene chloride, carbon disulfide, and dimethylformamide, slightly soluble in carbon tetrachloride and tetrahydrofuran, and insoluble in hydrocarbon solvents. Although a molecular weight determination by vapor phase osmometery in carbon disulfide suggests a monomeric structure in solution [calculated for S_4N_5Cl 234; found 222 (2.17 mg mL^{-1}), 228 (4.07 mg mL^{-1})]. The solid-state structure, as determined by X-ray crystallography, is polymeric (vide infra). The compounds S_4N_5F and $S_4N_5SbCl_6$ were readily prepared from S_4N_5Cl by the action of silver difluoride and antimony pentachloride, respectively, and were characterized by complete elemental analyses and by their vibrational spectra.

Table II. Selected Bond Angles (deg) in S_4N_5Cl

Angles at N and S within the $S_4N_5^+$ Cage			
S(1)-N(1)-S(2)	117.0 (3)	N(1)-S(2)-N(3)	108.7 (2)
S(1)-N(2)-S(3)	121.7 (2)	N(2)-S(3)-N(3)	119.5 (2)
S(2)-N(3)-S(3)	119.9 (2)	N(2)-S(1)-N(2)	102.7 (3)
N(1)-S(1)-N(2)	107.1 (2)	N(3)-S(2)-N(3)	99.1 (3)
Angles at S within the Unit of Four Sulfur Atoms			
S(2)-S(1)-S(3)	60.39 (4)	S(3)-S(2)-S(3)	90.87 (6)
S(3)-S(1)-S(3)	90.82 (7)	S(1)-S(3)-S(2)	59.18 (5)
S(1)-S(2)-S(3)	60.44 (4)		
Angle at Cl			
S(3)-Cl-S(3)	85.39 (6)		

Crystal Structure of S_4N_5Cl. The structure of S_4N_5Cl and important bond lengths are depicted in Figure 1. Selected bond angles are summarized in Table II, and the least squares planes and dihedral angles between these planes are given in

Table III. Weighted Least-Squares Planes and Dihedral Angles between Planes for S_4N_5Cl

Equation of Plane: $AX + BY + CZ - D = 0$[a]

plane no.	A	B	C	D	atom	X	Y	Z	dev, Å
1	−0.0758	−0.4267	−0.9012	−2.5289	S(3)[b]	2.0757	3.9579	0.7578	
					N(2)[b]	3.4386	3.2628	0.9723	
					N(3)[b]	0.7682	3.2394	1.2079	
					Cl	2.3034	5.8642	2.8114	−2.681
2	0.0000	0.0000	0.0000	0.0000	S(1)[b]	3.6079	1.9547	2.0037	
					S(2)[b]	0.8467	1.9547	2.3011	
					N(1)[b]	2.3081	1.9547	2.9996	
3	−0.0757	0.4269	−0.9011	−0.8607	S(3)[b]	2.0762	−0.0485	0.7576	
					N(2)[b]	3.4387	0.6466	0.9724	
					N(3)[b]	0.7679	0.6701	1.2080	
					S(1)	3.6079	1.9547	2.0037	−0.384
					S(2)	0.8467	1.9547	2.3011	−0.442
					N(1)	2.3081	1.9547	2.9996	−1.183

Dihedral Angles between Planes: 1-2, 90.0°; 1-3, 50.5°; 2-3, 90.0°

[a] *A*, *B*, *C*, and *D* are constants, and *X*, *Y*, and *Z* are orthogonalized coordinates. [b] Atoms in plane.

Table III. Figure 1 shows that the structure is predominantly ionic with $S_4N_5^+$ cations symmetrically bridged by Cl^- ions. It is interesting to compare this structure with that of the isoelectronic species $S_4N_5O^-$.[23] In the anion the exocyclic oxygen atom is bonded to a sulfur which is connected to three nitrogen atoms, whereas in S_4N_5Cl the chlorine atoms bridge sulfurs which are bonded to only two nitrogen atoms. The S–Cl distances are 2.81 Å, substantially longer than expected for a covalent S–Cl bond, e.g., 2.08 and 2.15 Å in $S_3N_3Cl_3$[22] or 2.17 Å in $S_3N_2Cl^+$, but close to the values observed for the distance of the Cl^- anion from the three S atoms of the cation (range 2.90–3.04 Å) in $S_3N_2Cl^+Cl^-$.[24] Andreasen and coworkers[25] have reported that the Cl^- ion is ca. 2.86 Å from both sulfur atoms of the five-membered ring in the $CCl_3CN_2S_2^+$ cation. They concluded that the S–Cl bonds are partially covalent in this and related compounds since a value of 3.6 Å is obtained for an ionic S^+–Cl^- bond by use of Pauling's formula[26] for calculating atomic radii and with the assumption that each sulfur atom has a charge of 0.5+ and the Cl^- ion has a charge of 1−. It seems reasonable to suggest, therefore, that there is partial covalent bonding in the S–Cl bonds of the S_4N_5Cl polymer. Indeed, the molecular weight data indicate that S_4N_5Cl behaves as a covalent monomer in carbon disulfide solutions. Furthermore, the SClS bond angle of ca. 85° is not inconsistent with partial covalent interaction between the chlorine atoms and the S_4N_5 cages.

The short S–N distances (1.545 and 1.558 Å) involving the S(3) atoms and the long-range interactions of these atoms with chlorine suggest some preferential localization of cation charge on these sulfur atoms. In contrast, the S–N distances involving S(1) and S(2) fall within the range 1.62–1.69 Å. As a result, the *average* S–N bond length (1.62 Å) is significantly longer than found in planar, monocyclic S–N cations, e.g., $S_3N_2^+$ (1.58 Å),[3a] $S_4N_3^+$ (1.55 Å),[4] and $S_5N_5^+$ (1.54–1.56 Å).[6]

$S_4N_5^+$ is the first example of a cationic S–N cage, and it is interesting to compare the S--S separations within the cage with the values found for the related anion $S_4N_5^-$ and for the neutral molecule S_4N_4. In S_4N_4, there are two S--S distances of 2.58 Å while the other four pairs of sulfur atoms are separated by 2.69 Å.[27] Indeed, Banister has pointed out that S_4N_4 can be regarded as a distorted tetrahedron of sulfur atoms with four of the edges bridged by nitrogens.[28] In the anion, $S_4N_5^-$, all six S--S distances fall within the narrow range 2.71–2.75 Å, giving an almost regular tetrahedron of sulfur atoms.[9] In contrast, five of the S--S separations in the cation, $S_4N_5^+$, are within the range 2.78–2.81 Å, while the sixth pair of sulfur atoms [S(3)] are 4.01 Å apart, i.e., a longer distance than the sum of the van der Waals radii for sulfur (ca. 3.50 Å). In a preliminary communication[8] we have adopted Banister's approach to rationalize the structures of $S_4N_5^-$ and $S_4N_5^+$. It was suggested that the 50 valence electrons of $S_4N_5^-$ can be accommodated by allocating a lone pair to each atom, a pair of electrons to each S–N bond, and an electron pair of higher energy to each S--S interaction in the S_4 tetrahedron. Thus, the existence of only five S--S interactions in $S_4N_5^+$, with 2 electrons less, is readily rationalized. In contrast, however, various molecular orbital calculations[29-33] allow the existence of only two transannular S–S bonds in S_4N_4. The need to develop a better understanding of the electronic structures of these ionic S–N cages, with particular reference to the significance of S--S distances, provided the major impetus for the ab initio HFS-SCF calculations on S_4N_4, $S_4N_5^-$, and $S_4N_5^+$ described below.

Table IV. Infrared and Raman Spectra of S_4N_5Cl, S_4N_5F, and $S_4N_5^+SbCl_6^-$ (cm^{-1})

S_4N_5Cl		S_4N_5F		$S_4N_5^+SbCl_6^-$	
IR	Raman	IR	Raman	IR	Raman
					1297 m
1140 w	1114 vw	1148 w			
1050 s		1043 s	1053 w	1059 s	1045 m
1023 m	1015 vs	1004 s		1012 m	
966 s	958 s	952 s	949 s	971 s	941 m
		879 m			
			838 m		840 w
800 w		800 w		810 w	
720 w	716 w	718 m	713 m	718 m	717 m
697 s		699 m		706 m	
	688 m				676 m
628 m		632 m	642 w	621 m	
584 s	587 w	591 s	612 m	588 s	598 w
560 sh		555 s	551 w	558 w	
		535 m			
481 m	474 m	481 w	482 s	482 m	485 s
462 m	457 sh	455 s		465 m	
422 m				416 m	
408 m	398 m	406 m	422 w	404 m	400 w
		348 m		350 vs	
308 w	304 m		324 m		333 s
				274 w	283 vw
			204 w		
	199 s				170 s
	173 w				130 vs

Vibrational Spectra of S_4N_5Cl, S_4N_5F, and $S_4N_5^+SbCl_6^-$. The infrared and Raman spectra of S_4N_5Cl, S_4N_5F, and $S_4N_5^+SbCl_6^-$ are summarized in Table IV. Although an excellent Raman spectrum was obtained for S_4N_5Cl, the quality of the spectra for the other two derivatives was poor. In the Raman spectrum of $S_4N_5^+SbCl_6^-$ the three bands at 333, 283, and 170 cm^{-1} can be readily assigned as ν_1 (A_{1g}), ν_2 (E_g) and ν_3 (T_{2g}) of an octahedral $SbCl_6^-$ ion (cf. 333, 293, and 175 cm^{-1} for the corresponding frequencies in S_2N^+-$SbCl_6^-$).[2] The very strong band at 350 cm^{-1} in the infrared

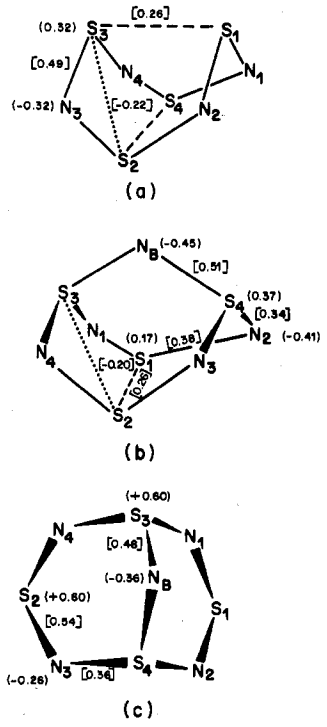

Figure 4. Overlap populations [brackets] and atomic charges (parentheses) in (a) S_4N_4, (b) $S_4N_5^-$, and (c) $S_4N_5^+$.

spectrum can be assigned to ν_3 of $SbCl_6^-$. Consideration of the other bands in the infrared spectrum of $S_4N_5^+SbCl_6^-$ reveals a very close similarity to the spectrum of S_4N_5Cl, consistent with the concept of an $S_4N_5^+$ cation in the chloride. Attempts to obtain the Raman spectrum of S_4N_5Cl in solution, in order to detect any structural changes from the solid state, were unsuccessful.

Although the infrared spectrum of S_4N_5F also shows the same general pattern as that of S_4N_5Cl, there are significant differences in the positions and relative intensities of the bands, particularly in the 950–1050-cm^{-1} region. The medium-intensity band observed at 879 cm^{-1} for S_4N_5F does not have a counterpart in the spectra of S_4N_5Cl or $S_4N_5^+SbCl_6^-$ and may be due to an S–F stretching vibration. Although it is not possible on the basis of the vibrational spectra to distinguish between the structural alternatives for S_4N_5F, (a) monomeric, (b) polymeric with symmetric fluorine bridging (cf. S_4N_5Cl), or (c) polymeric with asymmetric fluorine bridges, it does appear that the configuration of the S–N cage is not substantially different from that in S_4N_5Cl or $S_4N_5^+SbCl_6^-$.

The strong peak at 199 cm^{-1} in the Raman spectrum of S_4N_5Cl cannot be assigned to an S–S stretching vibration (cf. ν_{S-S} 213 cm^{-1} in S_4N_4)[34] since the calculations described below show that there are no S–S bonds in $S_4N_5^+$. It therefore seems likely that this band is associated with the symmetric stretching vibration of the S–Cl–S bridging unit.

Electronic Description of S_4N_4. Calculations of the electronic structure of S_4N_4 by extended-Hückel,[29] CNDO,[30,31] Xα–SW,[32] or semiempirical INDO-type ASMO–SCF[33] methods lead to essentially the same qualitative conclusions. All the methods indicate substantial S--S bonding for the two closest pairs of S atoms,[35] little or no N–N bonding, and polar S–N bonds. The INDO-type ASMO–SCF method predicts more polar bonds than the other methods.[33]

We have applied the HFS–SCF procedure to S_4N_4 both to compare our results with those of other methods and, more important, to provide a basis for our later description of $S_4N_5^-$ and $S_4N_5^+$. As Figure 4a shows, there is essentially no overlap population between adjacent nitrogen centers while that between the nearest-neighbor sulfur and nitrogens of 0.49 is comparable to that obtained for molecules in which the S–N linkage is commonly taken to be one bond. The overlap population between nearest sulfur pairs of 0.26 is thus suggestive of a "half-bond" while that between the more distant pair of sulfurs is –0.22.

From Figure 4a the atom charge, 0.32–, for each nitrogen indicates an excess of charge generated at the expense of valence electrons of the sulfur centers which now show a positive charge of 0.32+ (cf. q_N = 0.32– by the CNDO/BW procedure,[30] q_N = 0.56– from the SCF–Xα–SW method,[32] q_N = 0.47– by the CNDO/S method,[31] and q_N = 0.71– by the INDO-type ASMO–SCF method[33]). The experimental estimate for charge transfer from sulfur to nitrogen is $S^{0.6+}$–$N^{0.6-}$.[31] In summary, our calculations of overlap populations and charge distribution provide a description of S_4N_4 that is qualitatively in agreement with that found by other theoretical approaches. Specifically, S_4N_4 consists of a single bonded SN framework and two S--S bridge (partial) bonds with a substantial transfer of charge from sulfur to nitrogen.

In order to understand this picture in terms of its components we have calculated the overlap populations given in Table Va. Naturally one finds that a given MO makes contributions to the bonding for several different pairs of centers; furthermore, a particular orbital may be, e.g., antibonding for one region but bonding for another. For example, $2A_1$ is antibonding to the SN framework but bonding to the bridging sulfurs. Although it is not always possible to ascribe a single function to an MO as is normally done in the bonding, antibonding, and lone-pair assignments for diatomics, one can, failing that, give the principal shared functions. Thus, from Table Va we can say that for S_4N_4 the orbitals $1A_1$, 1E′, 1E″, $1B_1$, 2E′, 2E″, and $1A_2$ (E′ and E″ are used to distinguish the two components of the E representation) are all SN framework bonding orbitals but that one of the other low-lying orbitals, $1B_2$, has two principal functions, namely, bonding in the SN framework and bonding in the S--S bridge. In Table VI this assessment is displayed by indicating a pair of bonding electrons by ++ for, say, $1A_1$, 1E′, etc., a pair of antibonding electrons by –– (for $4A_1$), and the equally shared functions of the pair of bonding electrons of $1B_2$ by carrying a single + in the SN framework column and a single + in the S--S bridge column. In this way it can be seen that there are approximately 7.5 bonding and 1.5 antibonding SN framework orbitals for a net of 6 bonding orbitals spread over the 8 SN linkages. This is an average of 0.75 of a bond for each SN framework linkage—somewhat less than expected from the net overlap population of 0.48 but not unreasonable given the approximations inherent in such an assignment.

A similar analysis of the overlap contributions given in Table Va for the S--S bridge allows one to provide the assignment summarized in Table VI. We find bonding contributions equivalent to three pairs, i.e., 6 electrons (two of the orbitals involved, $2B_2$ and $3B_2$, are π-type orbitals). However, there are also antibonding contributions from 4E and a π^* orbital, 3E, for a total of 4 antibonding electrons. The result is a net of 2 bonding electrons, i.e., one bond, spread over two S--S bridge regions. We expect then a half-bond per region—a result which corresponds closely to the overlap population of 0.26. It should also be clear that it is the occupancy of the antibonding orbitals 3E and 4E which is responsible for the noticeably weakened S--S bridge bonds.

Indeed, if we examine the contributions of the MO's between the four distant S--S linkages, we find that only $2A_1$ is at all bonding in this region whereas $1B_2$, $3B_2$, and $4B_2$ are all antibonding. The result is a net of two antibonding contributions spread over the four distant S--S linkages (SS_{dist}), i.e., approximately "half an antibond" per linkage—corresponding well with the overlap population of –0.22. It should again be

Table V

(a) Orbital Overlap Populations in S_4N_4

MO designation	overlap pop., P_{ij}/orbital					
	$P_{NN_{adj}}$ [a]	$P_{SN_{adj}}$ [a]	$P_{SS_{bridge}}$ [b]	$P_{SS_{dist}}$ [c]	$P_{N_{self}}$ [d]	$P_{S_{self}}$ [d]
6E″		−0.021	−0.076	−0.002	0.122	0.273
6E′		−0.021	−0.076	0.002	0.122	0.273
$2A_2$	−0.013	0.009	−0.002		0.236	0.012
$4B_2$	0.004	0.002	0.048	−0.025	0.134	0.121
$4A_1$	0.003	−0.037	0.011	−0.002	0.171	0.202
$2B_1$	−0.003		−0.003	0.002	0.237	0.021
$3B_2$	0.001	−0.005	0.024	−0.026	0.041	0.250
5E″	−0.005	0.004	−0.001	0.002	0.140	0.117
5E′	−0.005	0.004	−0.001	0.002	0.140	0.117
4E″	0.001	−0.007	−0.030	0.006	0.187	0.104
4E′	0.001	−0.007	−0.030	0.006	0.187	0.104
3E″	0.002	0.005	−0.016	−0.005	0.055	0.190
3E′	0.002	0.005	−0.016	−0.005	0.055	0.190
$3A_1$	0.001	0.005	0.004		0.024	0.196
$2B_2$	0.003	0.012	0.027	0.004	0.046	0.112
$2A_1$	0.007	−0.022	0.051	0.015	0.126	0.152
$1A_2$	−0.003	0.022	−0.006	−0.008	0.086	0.099
2E″	−0.003	0.021	−0.007	−0.011	0.080	0.150
2E′	−0.003	0.021	−0.007	−0.011	0.080	0.150
$1B_2$	0.001	0.016	0.018	−0.020	0.024	0.183
$1B_1$	−0.011	0.024	−0.001	0.002	0.151	0.027
1E″	0.001	0.024	−0.002	0.004	0.086	0.057
1E′	0.001	0.024	−0.002	0.004	0.086	0.057
$1A_1$	0.005	0.022	0.004	0.005	0.069	0.057
$2\Sigma P_{ij}$	−0.013	0.244	0.128	−0.112	4.944	5.341

(b) Orbital Overlap Populations in $S_4N_5^-$ [e]

MO designation	N_B-S(4)	S(4)-N(2)	N(2)-S(1)	S(1)-S(2)	S(3)-S(4)
$6B_2$	−0.017	−0.031	0.009	0.002	+0.012
$9A_1$	−0.049	−0.007	−0.010	0.010	−0.005
$6B_1$	0.032	−0.002	−0.003	0.001	−0.002
$4A_2$		0.011	0.010	−0.001	
$8A_1$		−0.018	−0.023	0.052	−0.015
$3A_2$		0.003	0.002	−0.002	0.025
$7A_1$	0.034	−0.004	0.003	0.034	−0.038
$5B_2$	0.003	0.009	−0.006	−0.006	0.003
$5B_1$	0.022	−0.002	0.003	−0.009	
$6A_1$	−0.075	−0.023	−0.025	−0.002	−0.008
$4B_1$	0.006	−0.013	−0.007	−0.073	0.004
$4B_2$		0.005		0.002	0.006
$3B_1$	0.003	0.006	0.008	−0.015	
$5A_1$	0.006	0.005	0.001	0.016	
$4A_1$	−0.002	−0.010	0.003	0.044	0.020
$3B_2$	0.046	0.013	0.008	0.002	−0.005
$2A_2$		0.022	0.022		−0.007
$2B_1$	0.002	0.031	−0.016	−0.014	−0.010
$2B_2$	0.029	−0.020	0.028	0.002	−0.007
$3A_1$	−0.002	0.031	−0.003	0.012	−0.016
$1A_2$		0.021	0.021		0.016
$2A_1$	0.067	−0.004	0.019	0.006	0.006
$1B_1$		0.009	0.039	−0.004	0.002
$1B_2$	0.004	0.039	0.008		0.002
$1A_1$	0.016	0.021	0.016	0.002	0.005

(c) Orbital Overlap Populations in $S_4N_5^+$ [e]

MO designation	N_B-S(4)	S(4)-N(2)	N(2)-S(1)	S(1)-S(2)	
$6B_2$	−0.016	−0.060	−0.020		0.007
$6B_1$	0.029	0.001	−0.006		0.001
$8A_1$	−0.061	−0.001	−0.008	0.004	0.005
$4A_2$		0.005	0.008		0.010
$3A_2$		0.004	0.005		0.002
$5B_2$	0.004	0.012	0.011		0.001
$7A_1$	0.017	−0.008	0.005	0.008	−0.011
$5B_1$	0.023	−0.019	−0.023	−0.002	−0.005
$4B_2$	−0.001	0.024	0.005		0.001
$6A_1$	−0.050	−0.052	−0.052		0.014
$4B_1$	0.003	0.005	0.012	−0.006	0.003
$3B_1$	0.005	0.001	0.018	0.002	0.003
$5A_1$	0.002	0.003	0.019	0.002	0.001
$4A_1$	0.006	0.011	0.010	0.001	0.004

Table V (*Continued*)

MO designation	N_B-S(4)	S(4)-N(2)	N(2)-S(1)	S(1)-S(2)	S(3)-S(4)
$3B_2$	0.052	0.013	0.005		0.001
$2A_2$		0.026	0.018		0.009
$2B_1$	0.003	0.034	−0.016	−0.002	−0.011
$2B_2$	0.024	−0.013	0.029		0.005
$3A_1$	−0.008	0.032		0.001	−0.010
$1A_2$		0.017	0.025		0.002
$2A_1$	0.062	−0.004	0.023	0.001	−0.006
$1B_2$	0.006	0.036	0.009		0.002
$1B_1$	0.001	0.006	0.042		0.001
$1A_1$	0.021	0.018	0.017		0.002

[a] adj means adjacent. [b] SS_{bridge} refers to S_1–S_3 or S_2–S_4. [c] SS_{dist} refers to interactions between S atoms which are 2.70 Å apart. [d] self means self-atom overlap. [e] Refer to Figure 4 for atomic numbering scheme.

Table VI. Analysis of S_4N_4 Molecular Orbitals[a]

	dominant MO contribn[b,c]					dominant basis fcns	
	S	N		SS	SN		
MO designation	lp	lp	nb	bridge	framework	N	S
$2A_2$		11				$p_{x,y,z}$	
$4B_2$			1	+		p_z	$p_{x,y}$
$4A_1$					−−	s,p	s,p
$3B_2$			1	+		p_z	p_z
$2B_1$		11				s,p	
5E′	11						$p_{x,y}$
5E″		11				s,p	
4E′		11				s,p	
4E″				−−			s,p
3E′			1	−		$p_{x,y}$	p_z
3E″			1	−		$p_{x,y}$	p_z
$3A_1$	11						s,p
$2B_2$				++		$p_{x,y}$	p_z
$2A_1$				+	−	s,p	s,p
$1A_2$					++	p_z	$p_{x,y}$
2E′					++	s,p_z	s
2E″					++	s,p_z	s
$1B_2$				+	+	$p_{x,y}$	s
$1B_1$					++	s	$p_{x,y}$
1E′					++	s	s
1E″					++	s	s
$1A_1$					++	s	s

[a] lp means lone pair; nb means nonbonding. [b] 1 indicates an orbital with significant lone-pair or nonbonding character. 11 indicates an orbital which is essentially a lone pair or nonbonding orbital. A single + or a single − indicates an orbital with significant bonding (+) or antibonding (−) character. The ++ or −− entries indicate orbitals which are essentially bonding (++) or antibonding (−−). [c] Remember that the entires in this table are a useful, but *approximate*, compendium of the many entries given in Table Va.

emphasized that it is the occupancy of orbitals which are antibonding that destroys the possibility of a bond for this region. The lack of nearest-neighbor NN bonding is not, however, due to any such cancellation. As Table Va shows, the overlap populations of the occupied orbitals are uniformly small in the NN region.

In order to explain the atom charges we must consider not only the bonding/antibonding orbitals but also the nonbonding orbitals. For example, Table Va shows that the orbital $2B_1$ makes no contribution to any of the bonding regions we have considered. However, examination of the last two columns of Table Va, which contain the orbital overlap contributions to a single atomic center, N and S, respectively, indicates a significant contribution (0.237) to the N center but much less (0.021) to the sulfur center. Clearly $2B_1$ is a nitrogen-centered nonbonding orbital. Indeed, examination of the $s,p_{x,y}$ combinations shows it to be in the plane of the four nitrogens (p_x and p_y are in this plane) and to be directed outward from the set of four nitrogens. One can label $2B_1$ as a well-directed nitrogen lone pair. A careful analysis of $2A_2$, 5E′, and 4E′ reveals that they too are well-directed nitrogen lone pairs. Indeed, 4E′ is a planar lone pair like $2B_1$, but $2A_2$ and 5E′ are lone pairs directed away from the bonding region of the SN cage. Now although we have so far talked only of the SS bonding character of the $4B_2$, the $3B_2$, and the degenerate 3E levels, we can see from the last two columns of Table Va that they provide significant contributions to the nitrogen centers. One must conclude that, besides their SS bridge bonding properties, a shared function of $4B_2$, $3B_2$, 3E′, and 3E″ is that of nonbonding nitrogen-centered MO's. These orbitals are referred to as "nonbonding" rather than "lone pair" because they are largely p-type orbitals with less pronounced directional character away from the SN cage. For example, $3B_2$ and $4B_2$ are largely p_z on nitrogen whereas 3E′ and 3E″ are largely p_x, p_y, i.e., in-plane nonbonding. We summarize this analysis by showing, in Table VI, a pair of electrons "11" in the N lone-pair column for $2A_2$, $2B_1$, 5E″, and 4E′ and by inserting a single "1" for the shared nonbonding orbitals $4B_2$, $3B_2$, 3E′, and 3E″.

A similar analysis allows one to identify $3A_1$ and 5E′ as sulfur lone-pair orbitals. Once again we have a lone pair, $3A_1$, directed away from the cage and an in-plane lone pair 5E″ lying parallel to the plane of the four nitrogens.

Thus, we can say that there are four nitrogen lone-pair orbitals, giving 8 electrons on nitrogen, and a further four shared nonbonding orbitals which might reasonably be taken to contribute 4 more electrons on nitrogen centers. In addition there are 18 electrons involved in the SN framework orbitals (7.5 σ SN, 1.5 σ^* SN) which, on the basis of equal sharing, may be taken to provide 9 more electrons to the nitrogens. The total of 21 nitrogen electrons yields an excess of one charge distributed over four centers, an average of 0.25− per nitrogen center. This is reasonably close to the calculated value of 0.32−.

A similar summation for the sulfur centers gives a total of 23 electrons consisting of 4 electrons from the two sulfur lone pairs, 9 electrons as the sulfur share of the SN framework electrons, and 10 electrons from the orbitals forming the SS bridges. Thus, there is a deficiency of 1 electron spread over four sulfur centers or 0.25+ per center—again comparable to the calculated value.

In summary, the framework bonding contribution of the eight lowest MO's is reduced somewhat by occupancy of antibonding orbitals to give slightly less than one bond for each of the eight SN neighbors. There is weak SS bridge bonding, which occurs because the contributions of three occupied SS bonding orbitals are largely offset by two occupied antibonding orbitals. The ability of nitrogen to carry its valence electrons in nonbonding/lone-pair orbitals allows the existence of SN bonds which are stronger than the SS bonds. This same facility is responsible for the additional charge on nitrogen.

Although the foregoing analysis provides a reasonable rationalization of the bonding and charge distribution in S_4N_4, it must be remembered that the bonding/antibonding/lone-

pair language is a strong approximation in polyatomics. It is the numbers in Table Va which must be recognized as the basic description of the bonding.

Before we leave this section, it should be noted that the HOMO in S_4N_4 is a nitrogen lone-pair orbital, $2A_2$, but lying just below it is the orbital $4B_2$ without which there would be zero net S--S bridge bonding. Indeed, $4B_2$ is the HOMO according to calculations of the electronic structure of S_4N_4 by extended-Hückel (EH),[29] CNDO-S[31] or SCF-Xα-SW methods,[32] and some comment on this reversal of energy levels is therefore warranted. In fact, the heaviest involvement of d orbitals occurs for the $4B_2$ orbital (the d coefficients are 50% of the dominant p-type contributions), and it should be noted that the energy of this orbital is lowered relative to that of other orbitals when the sulfur d electrons are included in the basis set for EH or CNDO-S calculations.[31] Furthermore, it has been shown that inclusion of d functions in the basis set for SCF-Xα-SW calculations on S_2N_2 leads to a reversal of the energy levels for the top two occupied orbitals, $1B_{2g}$ and $1B_{3g}$.[32] It seems likely, therefore, that the lower energy of $4B_2$, relative to that of $2A_2$, found in this study is a direct consequence of the large d contribution to the $4B_2$ orbital. It might be expected that removal of a pair of electrons to give $S_4N_4^{2+}$ would destroy the S–S bridge bond, allowing the cage to open up. A separate calculation for $S_4N_4^{2+}$,[36] using one of the experimental geometries (d(S–N) = 1.55 Å; <NSN = 120°; <SNS = 150°),[5] shows that it is $4B_2$ which becomes a virtual orbital; the HOMO and LUMO remain the same as in S_4N_4.

The strongly antibonding character of the LUMO, 6E* (Table Va), with respect to the S--S bridge bond, suggests that the addition of a single electron to S_4N_4 would also have the effect of opening the cage. Indeed, a separate calculation (spin restricted) of $S_4N_4^-$, in the S_4N_4 geometry, shows a considerable weakening of the S–S bridge ([S–S_{bridge}] = 0.10). This result is in accord with the known behavior of the $S_4N_4^-$ radical anion,[37] which has been shown to be unstable above 0 °C *in solution* with respect to formation of the six-membered $S_3N_3^-$ ring,[38] apparently via a process involving intramolecular bond rupture.[38-40]

Electronic Description of $S_4N_5^-$. Figure 4b shows that the overlap population for the SN framework bonds in $S_4N_5^-$ is only 0.34–0.38, suggesting that the bond order for these bonds is less than 1. The overlap population (0.25) in the S--S bridge region suggests a half-bond, as in S_4N_4, while the overlap population of 0.51 in the SN_BS bridge (N_B denotes the nitrogen extra to the S_4N_4 parent system) is consistent with a single bond for these S–N bonds. The bond between the two sulfurs, S(3) and S(4), disappears (–0.03). The atom charges for $S_4N_5^-$ (Figure 4b) indicate that the four framework nitrogens carry among themselves over 1.5 electrons in addition to their valence electrons. About one-third of this is at the expense of the N^- entity inserted into the S_4N_4 system, and N_B is left with an excess of about 0.5 electron; the remaining nitrogen framework charge is extracted from the sulfurs, most of it coming from the sulfurs of the SN_BS bridge.

We shall attempt to rationalize the foregoing results on the basis of our knowledge of the S_4N_4 system. Clearly one of the SS bridges has the same overlap population (0.26 for S_1–S_2) as in S_4N_4. Indeed, examination of the overlap populations shows that it is formed in the same way: a σ-bonding contribution produced jointly by $4A_1$ and $8A_1$ (which arise from $2A_1$ and $2B_2$ in S_4N_4) and a shared π-bonding orbital $7A_1$ (arising from $3B_2$ in S_4N_4). As in S_4N_4 this is offset by the occupancy of an antibonding orbital $4B_1$ (arising from 4E) to give a net of a half-bond encompassing this S--S bridge region.

The SN_BS bridging unit can be viewed as an expansion of the S--S linkage of S_4N_4 by the addition of N^-. A pictorial description of the SN_BS bridge bonds is given in Figure 5, from which it can be seen that the s-type σ bond $1B_2$ of S_4N_4 now encompasses the bridging nitrogen and, using the 2s orbital of N_B, produces the very strong $2A_1$ bond of $S_4N_5^-$. As in S_4N_4, this bonding is reduced by the shared antibonding orbital $6A_1$* (which is the insertion of N_B into the framework orbital $4A_1$ of S_4N_4) to give a net of roughly half a bond. In addition it should be noted that the sulfur antibonding orbital 3E in S_4N_4 is *converted* by the insertion of N^- to $3B_2$, a strongly bonding orbital for SN_BS. Similarly the antibonding orbitals 5E and 6E are converted to the bonding orbitals $5B_1$ and $6B_1$, which together generate another SN_BS bonding pair of electrons. This dramatically strengthened bridge is reduced by about half a bond by the $9A_1$ orbital whose diffuse lone-pair distribution leaks over to become antibonding to the adjacent sulfurs. The net effect is about two bonds for the SN_BS bridge or one bond per S–N_B linkage. Figure 5 makes it clear that one should expect to find orbitals of $S_4N_5^-$ which are shifted dramatically from their position in S_4N_4 by the interaction with the atomic orbitals of N^-. To illustrate this, Figure 3 shows the energy levels of S_4N_4 and $S_4N_5^-$, taking the level $1A_1$ in each case as a common reference. The correlation lines are drawn strictly on the basis of symmetry. As this energy level diagram shows, most of the energy levels are unshifted. However, one can readily see that $2A_1$, $3B_2$, $6A_1$, and $6B_1$ are stabilized dramatically, while $5B_1$ is only shifted slightly ($3A_1$ is also stabilized and we will return to it later). A summary of the effect on energy levels of inserting N^- into the S_4N_4 system is given schematically in Figure 6.

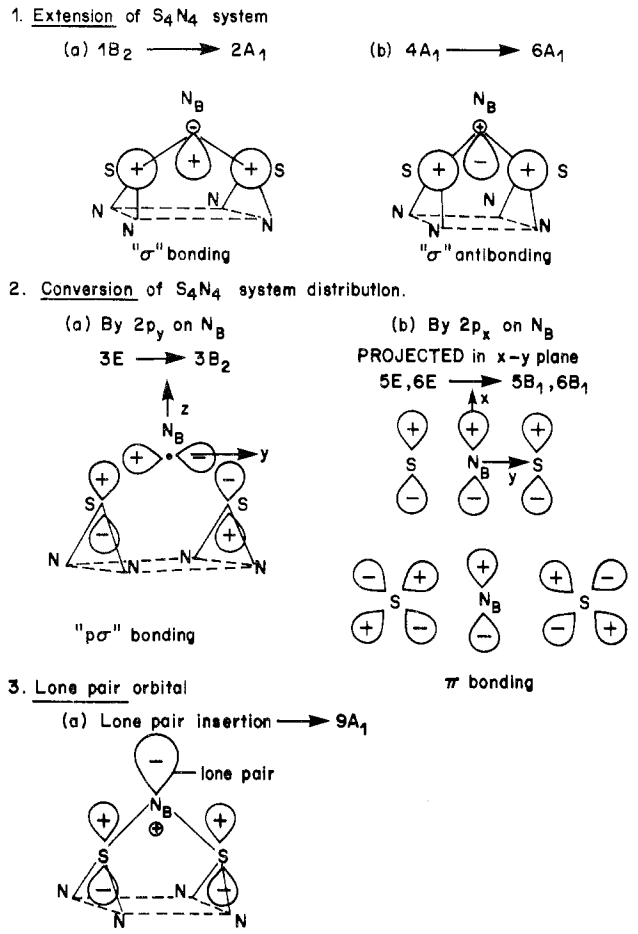

Figure 5. SN_BS bridging orbitals in $S_4N_5^-$.

Given this explanation of the SN_BS bridge bonding we can now turn to the rationalization of the weaker SN framework bonds in $S_4N_5^-$. Although a detailed examination of the orbital overlap contributions would show a number of subtle changes,

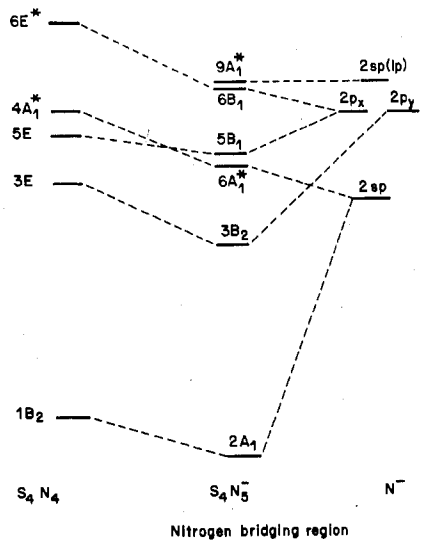

Figure 6. Stabilization of S_4N_4 levels by interaction with N^- "atomic" orbitals. The ordering, hybridization, and spacing of hybridized N^- orbitals are, of course, only illustrative.

there are two principal contributors. First, there is the loss of a bonding contribution as the $2B_2$ orbital stabilizes to $3A_1$ moving toward the bridging S--S region to become partially a S--S bridge nonbonding orbital (this also explains the reduced positive charge on these sulfurs). In addition to this loss of bonding contribution there is also an increase in antibonding character brought about by occupancy of $6B_2$* (arising from an antibonding 6E* virtual orbital of S_4N_4). The remaining orbitals of $S_4N_5^-$ have essentially the same function as in S_4N_4.

Before we leave this section, it should be noted that the bonding character of $6B_1$, the highest bonding orbital of $S_4N_5^-$ and a contributor to the SN_BS bridge, is due to a 3d contribution from the sulfur centers.

Electronic Description of $S_4N_5^+$. The bond overlap populations (Figure 4c) show that there is no S--S bond in $S_4N_5^+$. The SN_BS bridge bond is essentially the same as in $S_4N_5^-$. However, the framework bonds are altered significantly. The bonds furthest removed from the nitrogen bridge bond are strengthened, relative to $S_4N_5^-$, suggesting roughly 1 bond whereas the other framework bonds remain at somewhere near 0.75 bond. Perhaps the most striking feature is the additional shift in electron density away from the sulfur atoms, leaving residual charges of over 0.5 electron each. This charge is directed largely to the bridge nitrogen which goes from a deficiency of 1 electron (N^+) to an excess of about 0.33 electron. Of course, the framework nitrogens continue to carry a significant charge of about 0.25 electron.

The lack of a S--S bond in $S_4N_5^+$ is simply a consequence of the sulfur atoms being too far apart (ca. 4 Å). It seems likely that this is a result of the loss of the 2 electrons from the $8A_1$ orbital in $S_4N_5^-$, since without this orbital there would be no residual S--S bonding in $S_4N_5^-$. The loss of these 2 electrons permits the cage to open out in $S_4N_5^+$. It is also interesting to examine the change in the framework bonds as the cage opens. One finds that the same framework bonding orbitals as in $S_4N_5^-$ persist; however, there is in addition a conversion of nitrogen and sulfur nonbonding orbitals to weak framework bonds. For example, the orbitals $3B_1$ and $4B_2$ (which were framework nonbonding in $S_4N_5^-$ and framework nonbonding as 3E and 4E in S_4N_4) are now weakly bonding. The result would be a uniformly strengthened framework. However, the $6B_2$ orbital is strongly antibonding in the framework bond nearest the nitrogen bridge so that the net framework bond in this region is weaker. It should also be noted that the conversion of these sulfur nonbonding orbitals to framework bonds implies a transfer of electrons from sulfur to nitrogen, resulting in the increased positive charge on the sulfur centers.

Conclusion. The first cage (bicyclic) S–N cation has been prepared by the reaction of $S_3N_3Cl_3$ with $Me_3SiN{=}S{=}NSiMe_3$. An X-ray crystal structure determination of the product, S_4N_5Cl, reveals a polymeric structure in which $S_4N_5^+$ cations are symmetrically bridged by Cl^- anions. Ab initio HFS–SCF calculations of $S_4N_5^+$ and the related anion $S_4N_5^-$, show that introduction of the N^- entity into S_4N_4 destroys one of the transannular S–S bonds. The S–N bridge bonds which result are strong relative to the other S–N framework bonds in $S_4N_5^-$. In $S_4N_5^+$ there are no S–S bonds, as expected for loss of 2 electrons from the anion, $S_4N_5^-$. As a result $S_4N_5^+$ has an open cage structure which provides an opportunity to extend the S–N cage, for example by reaction with nucleophiles.

Acknowledgment. The authors are grateful to the National Research Council of Canada for support in the form of operating grants (T.C. and W.G.L.). Particular thanks are accorded Dr. Jan Troup of the Molecular Structure Corp., who carried out the X-ray structural determination of S_4N_5Cl.

Registry No. S_4N_5Cl, 67954-28-3; S_4N_5F, 71630-63-2; $S_4N_5SbCl_6$, 71606-72-9; $S_3N_3Cl_3$, 5964-00-1; $Me_3SiNSNSiMe_3$, 18156-25-7; $S_4N_5^+$, 71565-54-3; S_4N_4, 28950-34-7; $S_4N_5^-$, 58858-09-6.

References and Notes

(1) O. Glemser and W. Koch, *Angew. Chem., Int. Ed. Engl.*, **10**, 127 (1971).
(2) R. Faggiani, R. J. Gillespie, C. J. L. Lock, and J. D. Tyrer, *Inorg. Chem.*, **17**, 2975 (1978).
(3) (a) R. J. Gillespie, P. R. Ireland, and J. E. Vekris, *Can. J. Chem.*, **53**, 3147 (1975); (b) H. W. Roesky and A. Hamza, *Angew. Chem., Int. Ed. Engl.*, **15**, 226 (1976).
(4) T. N. Guru Row and P. Coppens, *Inorg. Chem.*, **17**, 1670 (1978), and references cited therein.
(5) R. J. Gillespie, D. R. Slim, and J. D. Tyrer, *J. Chem. Soc., Chem. Commun.*, 253 (1977).
(6) (a) H. W. Roesky, W. Grosse-Bowing, I. Rayment, and H. M. M. Shearer, *J. Chem. Soc., Chem. Commun.*, 735 (1975); (b) A. J. Banister, J. A. Durrant, I. Rayment, and H. M. M. Shearer, *J. Chem. Soc., Dalton Trans.*, 928 (1976).
(7) A. J. Banister, H. G. Clarke, I. Rayment, and H. M. M. Shearer, *Inorg. Nucl. Chem. Lett.*, **10**, 647 (1974).
(8) T. Chivers and L. Fielding, *J. Chem. Soc., Chem. Commun.*, 212 (1978).
(9) W. Flues, O. J. Scherer, J. Weiss, and G. Wolmershäuser, *Angew. Chem. Int. Ed. Engl.*, **15**, 379 (1976).
(10) G. A. Alange, A. J. Banister, and B. Bell, *J. Chem. Soc. A*, 2399 (1972).
(11) O. J. Scherer and R. Weiss, *Z. Naturforsch., B*, **25**, 1486 (1970).
(12) D. T. Cromer and J. T. Waber, "International Tables for X-ray Crystallography", Vol. IV, Kynoch Press, Birmingham, England, in press.
(13) D. T. Cromer and D. Liberman, *J. Chem. Phys.*, **53**, 1891 (1970).
(14) E. Clementi and C. Roetti, *At. Data Nucl. Data Tables*, **14**, 177 (1974).
(15) W. G. Laidlaw and M. Trsic, *Chem. Phys.*, **36**, 323 (1979).
(16) E. J. Baerends, D. E. Ellis, and P. Ros, *Chem. Phys.*, **2**, 41 (1973).
(17) T. Ziegler and A. Rauk, *Theor. Chim. Acta*, **46**, 1 (1977).
(18) J. Bojes, T. Chivers, W. G. Laidlaw, and M. Trsic, *J. Am. Chem. Soc.*, **101**, 4517 (1979).
(19) P. O. Offenhartz, "Atomic and M.O. Theory", McGraw-Hill, New York, 1970, displays formulas for orbital overlap population (eq 10.97), overlap population (eq 10.98), and net charge (eq 10.102).
(20) (a) O. J. Scherer and G. Wolmershäuser, *Angew. Chem., Int. Ed. Engl.*, **14**, 485 (1975); (b) J. Bojes, P. M. Boorman, and T. Chivers, *Inorg. Nucl. Chem. Lett.*, **12**, 551 (1976); (c) J. Bojes and T. Chivers, *Inorg. Chem.*, **17**, 318 (1978).
(21) See for example: O. J. Scherer and R. Wies, *Angew. Chem., Int. Ed. Engl.*, **10**, 812 (1971); **11**, 529 (1972); H. W. Roesky and H. Wieser, *ibid.*, **13**, 146 (1974).
(22) G. A. Wiegers and A. Vos, *Acta Crystallogr.*, **20**, 192 (1966).
(23) R. Steudel, P. Luger, and H. Bradaczek, *Angew. Chem., Int. Ed. Engl.*, **12**, 316 (1973).
(24) E. Zalkin, T. E. Hopkins, and D. H. Templeton, *Inorg. Chem.*, **5**, 1767 (1966).
(25) O. Andreasen, A. C. Hazell, and R. G. Hazell, *Acta Crystallogr., Sect. B*, **33**, 1109 (1977).
(26) L. Pauling, "The Nature of the Chemical Bond", 3rd ed., Cornell University Press, Ithaca, N.Y., 1960, pp 511–18.
(27) (a) M. L. DeLucia and P. Coppens, *Inorg. Chem.*, **17**, 2336 (1978); (b) B. D. Sharma and J. Donohue, *Acta Crystallogr.*, **16**, 891 (1963).
(28) A. J. Banister, *Nature (London), Phys. Sci.*, **239**, 69 (1972).

(29) A. G. Turner and F. S. Mortimer, *Inorg. Chem.*, **5**, 906 (1966).
(30) M. S. Gopinathan and M. A. Whitehead, *Can. J. Chem.*, **53**, 1343 (1974).
(31) W. R. Salaneck, J. W.-P. Lin, A. Paton, C. B. Duke, and G. P. Ceasar, *Phys. Rev. B*, **13**, 4517 (1976).
(32) D. Salahub and R. P. Messmer, *J. Chem. Phys.*, **64**, 2039 (1976).
(33) K. Tanaka, T. Yamabe, A. Tachibana, H. Kato, and K. Fukui, *J. Phys. Chem.*, **82**, 2121 (1978).
(34) J. Bragin and M. Evans, *J. Chem. Phys.*, **51**, 268 (1969).
(35) It should be noted that brief mention has recently been made of the possibility of four-center bonding involving all four sulfur atoms on the basis of electron density studies, which reveal an electron density peak of about 0.20 e $Å^{-3}$ in the center of the molecule between the two perpendicular S–S bonds (see ref 27a).
(36) M. Trsic and W. G. Laidlaw, to be submitted for publication.
(37) R. A. Meinzer, D. W. Pratt, and R. J. Myers, *J. Am. Chem. Soc.*, **91**, 6323 (1969).
(38) J. Bojes, T. Chivers, I. Drummond, and G. MacLean, *Inorg. Chem.*, **17**, 3668 (1978).
(39) J. D. Williford, R. E. Vanreet, M. P. Eastman, and K. B. Prater, *J. Electrochem. Soc.*, **120**, 1498 (1973).
(40) Fukui and co-workers have concluded that $S_4N_4^-$ has a lower energy than S_4N_4 on the basis of semiempirical INDO-type ASMO–SCF calculations. These authors suggest that S_4N_4 could be a useful electron acceptor in solid-state materials: K. Tanaka, T. Yamabe, A. Tachibana, H. Kato, and K. Fukui, *J. Phys. Chem.*, **82**, 2121 (1978).

Contribution from the Department of Chemistry,
North Carolina State University, Raleigh, North Carolina 27650

Emission Photoselection Studies of Transition-Metal Complexes. 1. Bis(diimine) Complexes

M. KEITH DEARMOND,* WEN LIANG HUANG, and CLIFFORD M. CARLIN

Received February 21, 1979

The technique of emission photoselection spectroscopy utilized with organic systems to determine nonradiative selection rules and orbital relaxation pathways has seldom been used with transition-metal systems. The ability of the technique to acquire polarization data for randomly oriented samples can be useful in clarifying some of the unique excited-state relaxation pathways (multiple-state emission) observed for these inorganic complexes. Therefore, a polarization spectrometer designed and assembled in this laboratory has been used to acquire emission and excitation polarization spectra for the three $[IrL_2Cl_2]^+$ complexes (where L is 2,2′-bipyridine (bpy), 1,10-phenanthroline (phen), and 5,6-dimethyl-1,10-phenanthroline (5,6-Mephen)), $[Ga(phen)_2Cl_2]^+$, and the three free ligands. The magnitude of the polarization, P, obtained for the three C_2 Ir(III) complexes and the free ligands indicates that these emission chromophores all behave as linear oscillators. The slope of the emission polarization found for the three Ir(III) complexes indicates the presence of two emitting states, consistent with an earlier suggestion of a charge transfer and dd* emission from these complexes. The polarization spectra for the three Ir(III) are similar; however, this result cannot alone be used to distinguish between assignment of the emission origin as either $d\pi^*$ (charge transfer) or $\pi\pi^*$ (ligand localized). The photoselection spectra of the Ga complex is depolarized, implying an intramolecular hopping of the localized excited state from ligand to ligand. The dominant intensity mechanism for the phosphorescence of the free ligands apparently is a second-order vibronic scheme involving an out-of-plane vibration while, as expected, a first-order spin–orbit mechanism is utilized with the transition-metal complexes.

Introduction

Typically, the relaxation of excited states for complex organic molecules has been rationalized from a combination of emission and absorption spectra, decay times, and quantum yields.[1,2] A substantial body of such experimental data accumulated for aromatic hydrocarbon and heterocyclic molecules has permitted generation of detailed and sophisticated theories[3,4] describing the nonradiative processes in these systems by emphasizing the role of molecular vibrations in these deactivation processes. A successful subsidiary effort for light-atom organic systems has utilized the emission photoselection technique[5] to determine nonradiative selection rules[6,7] and orbital relaxation pathways[8] for aromatics and heteroaromatics.

From these data and theories, some simple and useful generalizations concerning relaxation of excited states of organic aromatics have been elaborated. (1) Fluorescence (spin-allowed emission) typically occurs from the vibrationless state of the lowest excited singlet level (and only this state) irregardless of the excitation energy. (2) A single phosphorescence (spin-forbidden emission) typically occurs from the lowest vibrational state of the lowest excited triplet state. (3) Intersystem crossing (singlet to triplet nonradiative processes) typically occurs only from the lowest singlet electronic state, since vibrational relaxation from higher excited singlets called "internal conversion" is extremely rapid. As a consequence, emission quantum yields are typically wavelength independent. (4) Molecular vibrations of the emitter can function as either acceptors or activators in the nonradiative deactivation of excited states.[3,8]

Construction of an appropriate detailed theory of the excited state for transition-metal complexes necessitates accumulating sufficient emission data for a large number of structurally related complexes. Only two metal ion configurations, d^3 and d^6, are found to luminescence in a number of complexes.[9,10] For the d^3 Cr^{3+} systems, a weak luminescence occurs from dd* states, most commonly a line like phosphorescence from the excited ^2E state.

For the d^6 configuration, complexes of Ru^{2+}, Os^{2+}, Rh^{3+}, and Ir^{3+} provide examples of not only dd* type emission but also emission from ligand localized $\pi\pi^*$ and charge-transfer states,[11] metal to ligand type. Here the different types of emitting states and the range of spin–orbital coupling schemes exceed that for either the d^3 configuration or the organic emitters; consequently unusual behavior becomes more common. For example, the intense "phosphorescent" emission of a number of diimine complexes of Ru^{2+} and Ir^{3+} is measurable at room temperature. Moreover the temperature variation of the intensity and lifetime of the $[Ru(bpy)_3]^{2+}$ and $[Ru(phen)_3]^{2+}$ complexes varies in a manner indicating that a manifold of close-lying thermally equilibrated states of common orbital origin produces the emission.[12,13] Further, wavelength-dependent quantum yields[14] and laser rise-time experiments[15] imply that upper level intersystem crossing occurs. Such phenomena imply (1) that upper level intersystem crossing can compete with internal conversions for these ma-

0020-1669/79/1318-3388$01.00/0